

Chaperone Priming of Pilus Subunits Facilitates a Topological Transition that Drives Fiber Formation

Frederic G. Sauer,^{1,6} Jerome S. Pinkner,¹
Gabriel Waksman,^{2,3,4,5} and Scott J. Hultgren¹

¹Department of Molecular Microbiology

²Department of Biochemistry and Molecular
Biophysics

Washington University Medical School

660 South Euclid Avenue

St. Louis, Missouri 63105

³Birkbeck College

Department of Crystallography

Malet Street

London

WC1E 7HX, UK

⁴The Ludwig Institute for Cancer Research

University College London

91 Riding House Street

London

W1W 7BS, UK

Summary

Periplasmic chaperones direct the assembly of adhesive, multi-subunit pilus fibers that play critical roles in bacterial pathogenesis. Pilus assembly occurs via a donor strand exchange mechanism in which the N-terminal extension of one subunit replaces the chaperone G₁ strand that transiently occupies a groove in the neighboring subunit. Here, we show that the chaperone primes the subunit for assembly by holding the groove in an open, activated conformation. During donor strand exchange, the subunit undergoes a topological transition that triggers the closure of the groove and seals the N-terminal extension in place. It is this topological transition, made possible only by the priming action of the chaperone that drives subunit assembly into the fiber.

Introduction

Urinary tract infections (UTIs) are among the most common bacterial infections of humans, second only to respiratory infections (Sussman, 2001). They include both kidney and bladder infections (pyelonephritis and cystitis, respectively) and have been estimated to account for 100,000 hospital admissions and eight million physician office visits annually in the United States alone (Warren, 1996). Urinary tract infections primarily affect women—it has been estimated that 50% of women will experience at least one UTI during their lives, and that 20%–40% of these will develop one or more recurrent infections (Stanton and Dwyer, 2000; Hooton, 2000). Uropathogenic *E. coli* (UPEC) is the most common cause of UTIs (Muhldorfer et al., 2001). UPEC organisms express on their surfaces various multi-subunit fibers termed pili

that have been shown to be critical for the establishment of urinary tract infections (Roberts et al., 1994; Connell et al., 1996; Mulvey et al., 1998). These pili mediate bacterial attachment to host tissues, an essential early step in UTI pathogenesis (Hultgren et al., 1996). Pilus-mediated attachment facilitates bacterial colonization and triggers a complex web of events, including signaling in both the bacterium and host, that then influences the course and outcome of the infection (Mulvey et al., 1998; Martinez et al., 2000; Hung et al., 2001).

P pili are expressed by many strains of uropathogenic *E. coli*. These pilus fibers are encoded by the *pap* gene cluster (*papA-K*) and bind to the globoseries of glycolipids present in the human kidney (Hull et al., 1981; Lund et al., 1987). P pili have been shown to be required for the establishment of pyelonephritis (Roberts et al., 1994). Each P pilus consists of a thick, rigid rod with a thinner, more flexible tip fibrillum at its distal end. The rod contains PapA subunits arranged to form a tightly wound, hollow, right-handed helical structure (Gong and Makowski, 1992; Bullitt and Makowski, 1995). The tip fibrillum contains PapE subunits arranged in a more open helical conformation (Kuehn et al., 1992). The PapG adhesin, which binds the glycolipid receptor, is at the distal end of the tip fibrillum (Kuehn et al., 1992; Dodson et al., 2001). The PapF and PapK pilus subunits are thought to link the PapG adhesin to the tip fibrillum and the tip fibrillum to the rod, respectively (Jacob-Dubuisson et al., 1993).

P pili are members of a large family of bacterial surface fibers that are assembled by a conserved secretion and assembly system termed the chaperone-usher pathway (Thanassi et al., 1998a). This chaperone-usher pathway participates in the assembly of surface organelles in many pathogenic bacteria, including uropathogenic and enterotoxigenic *E. coli*, *Haemophilus influenzae*, *Klebsiella pneumoniae*, *Proteus mirabilis*, *Bordetella pertussis*, and *Salmonella* and *Yersinia* species, including *Yersinia pestis*, the causative agent of bubonic plague (Hung et al., 1996). A periplasmic chaperone and an outer-membrane usher direct the assembly of each such organelle. PapD and PapC are the chaperone and usher, respectively, for P pili. During pilus assembly, each subunit interacts with the chaperone to form a stable chaperone-subunit complex in the periplasm (Lindberg et al., 1989). Each pilus subunit has an incomplete immunoglobulin-like (Ig) fold that lacks its seventh, C-terminal β strand, resulting in a hydrophobic groove on its surface where this missing strand would otherwise be. The chaperone contributes a portion of its G₁ strand to complete the subunit Ig fold by occupying the groove. This so-called donor strand complementation interaction couples the folding of the subunit with the transient capping of its interactive groove and thus ensures that the groove is never prematurely exposed to make non-productive or aggregative interactions (Choudhury et al., 1999; Sauer et al., 1999; Barnhart et al., 2000). Dissociation of the chaperone-subunit complex precedes the incorporation of the subunit into the pilus fiber, which grows from the base. In the chaperone-subunit complex,

⁵ Correspondence: waksman@biochem.wustl.edu

⁶ Present address: Section of Microbial Pathogenesis, Yale University School of Medicine, New Haven, Connecticut 06536

Table 1. Data Collection and Refinement

| Data Collection | | | | | | |
|--------------------------------|--------------------------------------|---|--------------------------|------------|------------------|------------------|
| Data Set | Radiation (Å) | Resol. (Å) | Total/Unique Reflections | I/σ(I) | Completeness (%) | R _{sym} |
| PapEK SeMet peak | 0.9793, APS 19-ID | 30–1.87 | 240,454/35,128 | 21.1 (4.0) | 94.0 (79.8) | 0.053 (0.218) |
| PapEK SeMet remote | 0.9667, APS 19-ID | 30–1.87 | 232,749/18,969 | 33.8 (8.4) | 99.2 (96.8) | 0.050 (0.149) |
| FOM (30–1.87 Å): | 0.25 | | | | | |
| PapDE SeMet 1 | CuKα, Raxis | 30–2.3 | 162,110/27,884 | 28.7 (6.5) | 91.0 (91.5) | 0.041 (0.175) |
| PapDE SeMet 2 edge | 0.9782, APS 19-BM | 30–2.6 | 165,765/35,518 | 16.6 (2.3) | 78.8 (69.8) | 0.034 (0.181) |
| PapDE SeMet 2 peak | 0.9780, APS 19-BM | 30–2.6 | 162,686/36,150 | 17.8 (2.6) | 80.7 (74.6) | 0.033 (0.157) |
| PapDE SeMet 2 remote | 0.9667, APS 19-BM | 30–2.6 | 168,801/34,618 | 13.3 (1.8) | 76.4 (54.7) | 0.040 (0.227) |
| FOM (30–2.6 Å): | 0.48 | | | | | |
| Refinement | | | | | | |
| | PapE _{Ntd} K _{Nte} | PapD _{His} PapE _{Ntd} | | | | |
| Data Set | PapEK SeMet remote | PapDE SeMet 1 | | | | |
| Resolution (Å) | 30–1.87 | 30–2.3 | | | | |
| Total Reflections | 18937 | 27882 | | | | |
| Test Set | 1109 | 2020 | | | | |
| Working Set | 17828 | 25862 | | | | |
| Atoms | 2395 | 5228 | | | | |
| Water Atoms | 140 | 164 | | | | |
| R _{free} | 0.249 | 0.279 | | | | |
| R | 0.208 | 0.226 | | | | |
| RMSD Bonds (Å) | 0.0054 | 0.0061 | | | | |
| RMSD Angles (deg.) | 1.22 | 1.29 | | | | |
| Average B-factor | 19.9 | 39.7 | | | | |
| RMSDB (main) (Å ²) | 1.6 | 1.6 | | | | |
| RMSDB (side) (Å ²) | 2.3 | 2.3 | | | | |

Values for high-resolution shell in parentheses. Completeness for $I/\sigma(I) > 0$. $R_{sym} = \sum |I - \langle I \rangle| / \sum I$, where I = observed intensity and $\langle I \rangle$ = average intensity of multiple observations of symmetry-related reflections. FOM = Figure of merit. $R = \sum |F_o - F_c| / \sum F_o$. R_{free} is calculated for test set reflections randomly excluded from refinement. Bond and angle deviations (RMSD) are from ideal values; B-factor deviations are between bonded atoms.

PapE that lacks its N-terminal extension (residues 2 to 12 [Figure 1A]; we termed the mutant “N-terminal-deleted PapE” or “PapE_{Ntd}”). Purified PapE_{Ntd} in complex with PapD_{His} (PapD_{His}PapE_{Ntd}) does not form multimers when incubated at room temperature in 2% SDS and subjected to SDS-PAGE (Figure 1B, lanes 3 and 4). Thus, the N-terminal extension is required for PapE-PapE interactions.

In the pilus, the N-terminal extension of PapK is thought to bind to the groove of the PapE subunit at the base of the tip fibrillum. The addition of an ~15-fold molar excess of peptide corresponding to the N-terminal extension of PapK (“K_{Nte}”, residues 1–11 of the mature protein [Figure 1A]) to purified PapD_{His}PapE_{Ntd} yields an additional species as shown by incubation of the sample in 2% SDS at room temperature before SDS-PAGE (Figure 1B, lane 6). This species was shown to contain PapE_{Ntd} and the K_{Nte} peptide by mass spectrometry and N-terminal sequencing. Thus, the K_{Nte} peptide triggers donor strand exchange, displacing the chaperone from the PapD_{His}PapE_{Ntd} chaperone-subunit complex to form a PapE_{Ntd}K_{Nte} subunit-peptide complex. This latter complex runs above its expected molecular weight when incubated in 2% SDS at room temperature and subjected to SDS-PAGE because it is not fully dissociated or denatured (Figure 1B, lanes 6 and 8). When the PapE_{Ntd}K_{Nte} subunit-peptide complex is incubated in 2% SDS at 95°C before SDS-PAGE, the complex dissociates, the peptide runs off the gel, and only the PapE_{Ntd} band remains (Figure 1B, lanes 5 and 7). This resistance to dissociation in SDS at room temperature but not at 95°C confirms the wild-type character of the interaction in the

PapE_{Ntd}K_{Nte} complex (Soto et al., 1998; Striker et al., 1994).

To further characterize the role of the chaperone in donor strand exchange, we added PapD_{His}PapK chaperone-subunit complexes to either PapD_{His}PapE_{Ntd} or PapE_{Ntd}K_{Nte} complexes. The addition of PapD_{His}PapK to PapD_{His}PapE_{Ntd} results in donor strand exchange; PapK, still bound to its PapD_{His} chaperone, displaces the PapD_{His} chaperone bound to PapE_{Ntd} to yield a PapD_{His}PapKPapE_{Ntd} chaperone-subunit-subunit complex. This complex resolves into PapD_{His} and a PapKPapE_{Ntd} subunit-subunit complex, as verified by N-terminal sequencing, upon incubation in 2% SDS at room temperature followed by SDS-PAGE (Figure 1C, lane 1). In contrast, the addition of PapD_{His}PapK to PapE_{Ntd}K_{Nte} does not result in donor strand exchange (Figure 1C, lane 2). The N-terminal extension of the full-length PapK does not displace the PapK N-terminal extension peptide already in the PapE_{Ntd} groove, and thus, no PapK PapE_{Ntd} subunit-subunit complex is formed. Instead, the PapE_{Ntd}K_{Nte} subunit-peptide complex remains intact (Figure 1C, lane 2). Thus, donor strand exchange only occurs when the PapE_{Ntd} subunit is bound to the chaperone. These results indicate that the chaperone primes the subunit to interact with the N-terminal extension of the next subunit in the pilus during fiber assembly.

High-Resolution Structures of Subunit Complexes Before and After Donor Strand Exchange

To elucidate the structural basis for chaperone priming of the subunit during fiber assembly, we determined the

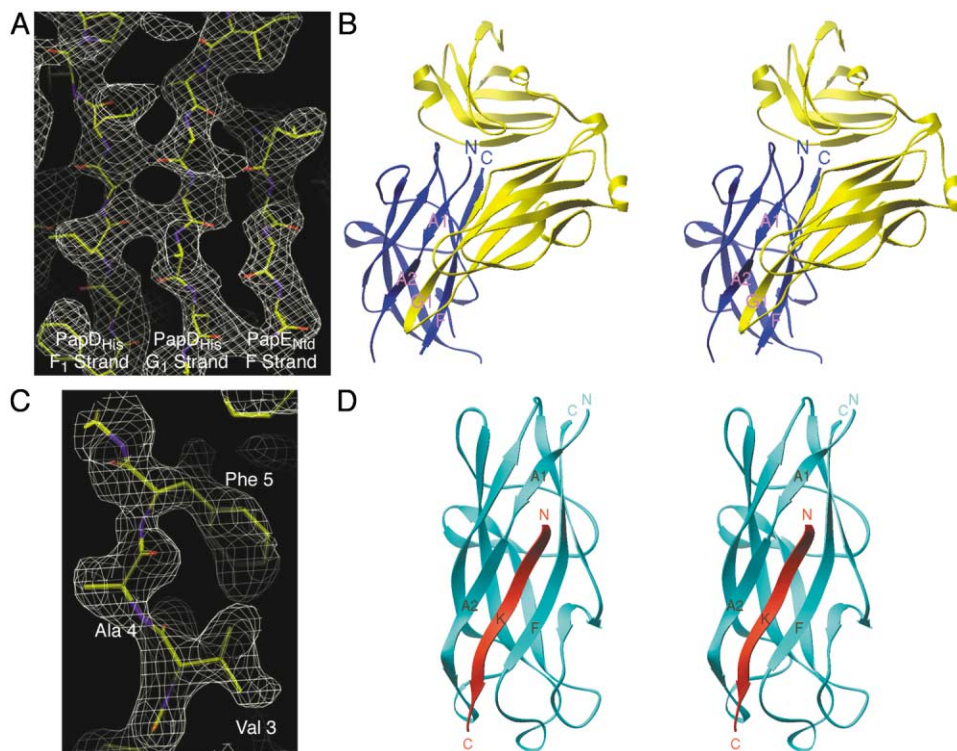


Figure 2. PapD_{His}PapE_{Ntd} and PapE_{Ntd}K_{Nte} Crystal Structures

(A) Electron density of the PapD_{His}PapE_{Ntd} complex from a map calculated using density-modified experimental MAD phases to 2.6 Å resolution. Carbons, nitrogens, and oxygens of the model are indicated in yellow, blue, and red, respectively. Strands are labeled. (B) Stereo ribbon diagram of the PapD_{His}PapE_{Ntd} complex. PapD_{His} is in yellow and PapE_{Ntd} is in blue. The N and C termini of PapE_{Ntd} are labeled in blue. The PapD_{His} G₁ and PapE_{Ntd} A1, A2, and F strands are labeled in magenta. (C) Electron density of PapE_{Ntd}K_{Nte} from a map calculated using density-modified experimental SAD phases to 1.87 Å. Color-coding and representation of the model are as in (A). Residues of PapK_{Nte} are labeled. (D) Stereo ribbon diagram of the PapE_{Ntd}PapK_{Nte} complex. PapE_{Ntd} is in cyan; PapK_{Nte} is in red and labeled with a K. The N and C termini of PapE_{Ntd} and PapK_{Nte} are indicated in cyan and red, respectively. The A1, A2, and F strands of PapE_{Ntd} are labeled.

crystal structures of the PapD_{His}PapE_{Ntd} and PapE_{Ntd}K_{Nte} complexes to 2.3 Å and 1.87 Å, respectively (Table 1, Figure 2). By providing high-resolution views of the PapE subunit before and after donor strand exchange, these structures reveal the mechanism of chaperone priming. The PapD_{His}PapE_{Ntd} complex exhibits the donor strand complementation interaction characteristic of chaperone-subunit complexes (Figure 2B) (Choudhury et al., 1999; Sauer et al., 1999). The G₁ strand of PapD_{His} (residues 101–112) completes the PapE_{Ntd} Ig fold by occupying the groove between the subunit A2 and F strands (Figures 2B and 3). Donor strand complementation produces a distinctive non-canonical Ig fold, since the chaperone G₁ strand runs parallel to, rather than anti-parallel to, the subunit F strand (Figures 2B and 3) (Choudhury et al., 1999; Sauer et al., 1999). In the PapE_{Ntd}K_{Nte} complex, the K_{Nte} peptide has replaced the chaperone G₁ strand. The K_{Nte} peptide runs anti-parallel to the PapE_{Ntd} F strand, in the opposite direction as does the G₁ strand in the PapD_{His}PapE_{Ntd} complex, and produces a perfectly canonical Ig fold (Figures 2D and 3). Thus, during donor strand exchange, the subunit undergoes a topological transition from a non-canonical to a canonical Ig fold.

Donor Strand Exchange Produces a Shift in Register in the Complementing Strands
Superposition of the structures of PapE_{Ntd} with their complementing strands reveals that in addition to running in opposite directions, the G₁ strand and N-terminal extension are shifted in register relative to each other (Figure 4A). There are five positions in the groove, designated for convenience P1–P5, at which residues of the complementing strands interact with the subunit (Figures 1A, 4B, and 5). In the PapD_{His}PapE_{Ntd} structure, the chaperone G₁ strand occupies P1–P4, while in the PapE_{Ntd}K_{Nte} structure, the N-terminal extension peptide occupies P2–P5. The respective registers of the G₁ and N-terminal extension strands are determined by the steric complementarity between the P1–P5 groove positions and the side chains that occupy them. In the PapD_{His}PapE_{Ntd} chaperone-subunit complex, Leu 107, Ile 105, and Leu 103 respectively of the G₁ strand occupy the relatively deep positions P1–P3. The P4 position is very shallow, as Phe 138 of PapE_{Ntd} protrudes out of the groove at this point (Figures 4B and 5C). P4 is occupied by Asn 101, the final residue at this end of the G₁ strand of PapD. However, rather than projecting into the groove,

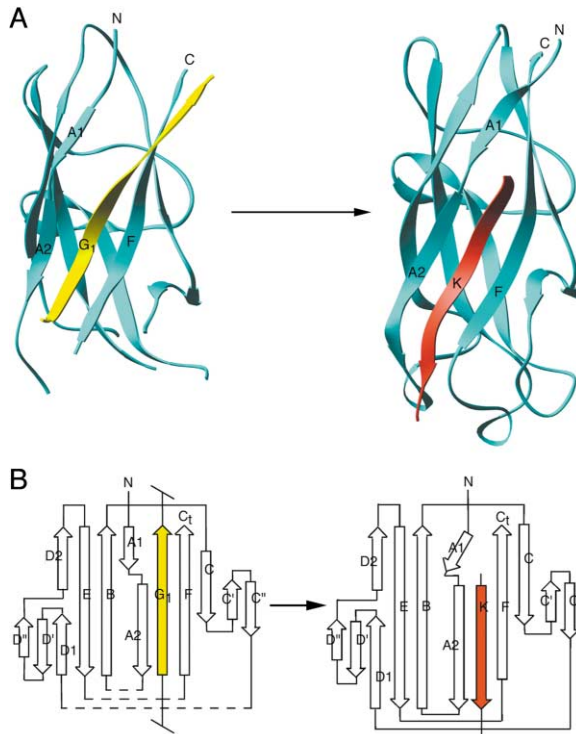


Figure 3. Donor Strand Exchange at High Resolution

(A) Ribbon diagrams of PapE with complementing strands before (left, from the PapD_{His}-PapE_{Ntd} complex) and after (right, from the PapE_{Ntd}-K_{Nte} complex) donor strand exchange. PapE_{Ntd} is in cyan, the chaperone G₁ strand is in yellow, and the K_{Nte} peptide is in red. The N and C termini and the A1, A2, and F strands of PapE_{Ntd} are labeled. Note the positions of the N and C termini of PapE_{Ntd} before (open groove) and after (closed groove) donor strand exchange.

(B) Donor strand exchange topology. Arrows indicate strands. In the chaperone-subunit complex (left), the chaperone G₁ strand (yellow) runs parallel to the PapE_{Ntd} F strand to complete its Ig fold in a non-canonical manner. After donor strand exchange (right), the PapK N-terminal extension (red) runs anti-parallel to the F strand to yield a canonical Ig fold. Dashed lines indicate disordered regions and the diagonal lines at either end of the chaperone G₁ strand indicate additional protein not shown.

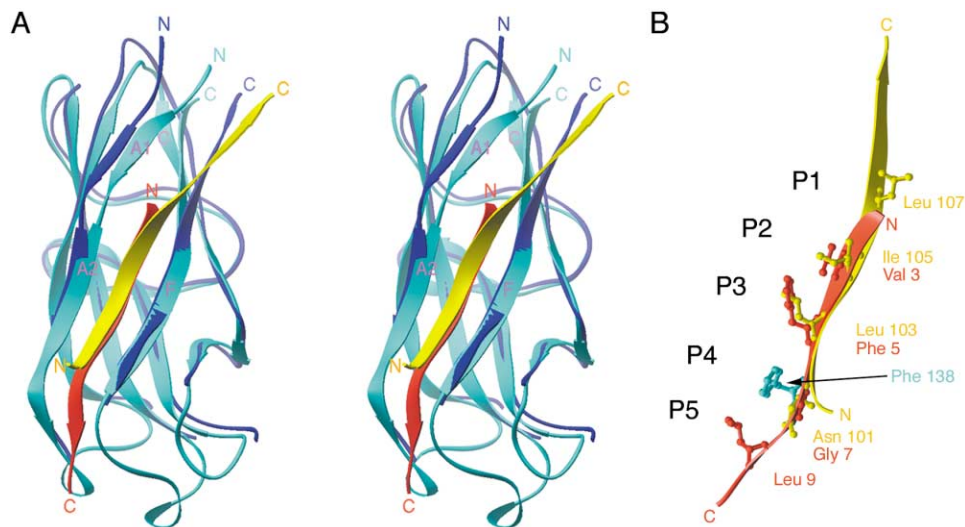


Figure 4. Superposition of Subunit Complexes and Definition of Positions P1-P5

(A) Stereo view of the superposition of the PapE_{Ntd}-K_{Nte} (cyan and red, respectively) and PapD_{His}-PapE_{Ntd} (yellow and blue, respectively) complexes. Only the G₁ strand (residues 100–112) of PapD_{His} is shown. The various N and C termini are indicated in the same color scheme as the ribbons. Strands of PapE_{Ntd} from the PapE_{Ntd}-K_{Nte} complex are indicated in magenta. Note particularly the positions of the PapE_{Ntd} N and C termini in the more open position (blue) when in complex with PapD_{His} and in the more closed position (cyan) when in complex with the K_{Nte} peptide. The opposite orientation and shift in register of the two complementing strands is easily appreciated.

(B) Definition of positions P1-P5 at which residues from the complementing strands interact with the hydrophobic groove of PapE_{Ntd}. Superposition of the chaperone G₁ strand (yellow) and the K_{Nte} peptide (red) rotated roughly 90° about a vertical axis from the view in (A). The base of subunit groove (not shown except for the Phe 138 side chain [cyan]) is on the left. The positions are indicated (P1-P5) and the side chains are shown and labeled, color-coded as the strands. The protruding Phe 138 of PapE_{Ntd} that makes P4 very shallow is shown in cyan. The N and C termini of the strands are indicated, color-coded as the ribbons. Note that the N terminus of the G₁ strand begins to curve away from the groove at P4, allowing the Asn 101 side chain here to run parallel to the groove rather than project into it.

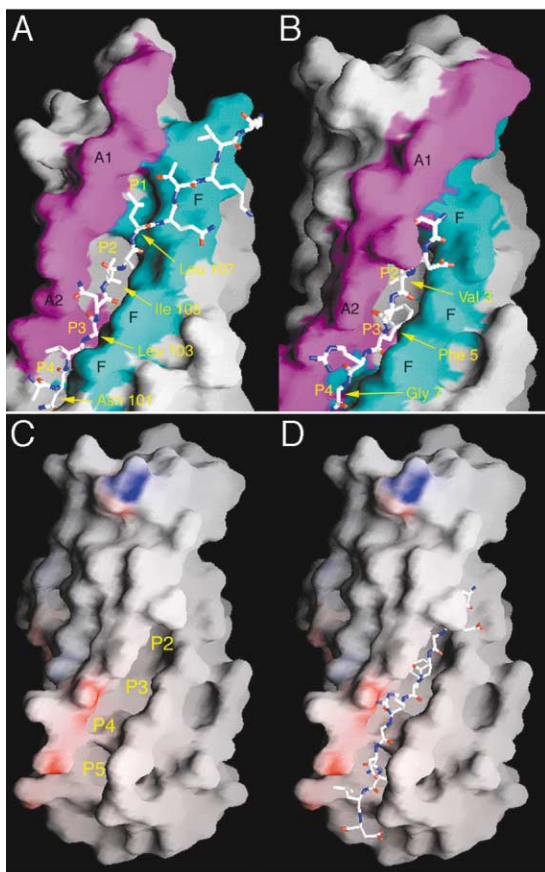


Figure 5. Open and Closed Conformations of the Groove
 (A) and (B) Close-up views of the open (PapD_{His}PapE_{Ntd}, A) and closed (PapE_{Ntd}K_{Nte}, B) conformations of the PapE_{Ntd} groove. In both (A) and (B), PapE_{Ntd} is shown in surface representation, with the A1 and A2 strands in magenta and labeled and the F strand in cyan and labeled. The G₁ (A) and K_{Nte} (B) strands are in stick representation, color-coded white, blue, and red for carbon, nitrogen, and oxygen, respectively. P1-P4 and the residues that occupy them are labeled in yellow. Note the closure of the groove (compare magenta and cyan surfaces in the two images).
 (C) and (D) Surface representations of the closed conformation of PapE_{Ntd} from the PapE_{Ntd}K_{Nte} complex. In (C), the surface is shown without the K_{Nte} peptide, color-coded red and blue for negative and positive charge, respectively. Positions P2-P5 are indicated in yellow; P1. Note the shallowness of position P4. In (D), the PapK_{Nte} strand is added in stick representation, colored coded as in (A) and (B). Note the snug fit of the N-terminal extension in the subunit groove.

where there is no room for it, the Asn 101 side chain runs parallel to the groove (Figure 4B). In the PapD_{His}PapE_{Ntd} subunit-peptide complex, the region around P5 is disordered and not visible (Figure 4A). In the PapE_{Ntd}K_{Nte} complex, Val 3 and Phe 5 of the K_{Nte} peptide occupy the relatively deep P2 and P3 positions, respectively. The small Gly 7 of K_{Nte} fits into the shallow P4 position on top of Phe 138, and Leu 9 of the K_{Nte} peptide occupies the relatively deep P5 position (Figure 4B). Presumably the interactions of Leu 9 of K_{Nte} with hydrophobic residues in the core of PapE_{Ntd} here contribute to the ordering of this region. Gly 5 is conserved in P pilus subunits (Figure 1A); the bulky character of the residue at the

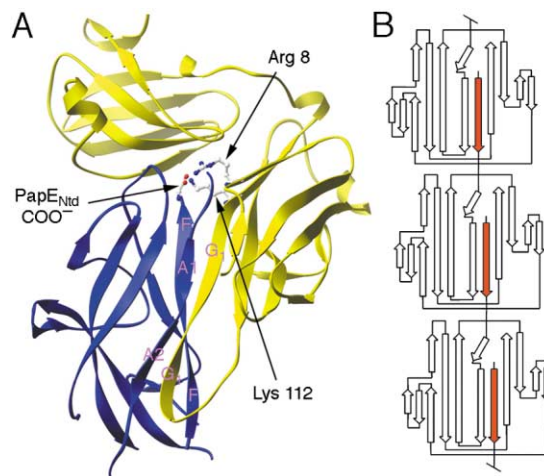


Figure 6. Anchoring Interaction in the Chaperone Cleft and a Model of Subunits in a Pilus
 (A) Ribbon diagram of the PapD_{His}PapE_{Ntd} complex. PapD_{His} is in yellow, PapE_{Ntd} is in blue. Strands are labeled in magenta. The conserved Arg 8 and Lys 112 residues in the chaperone cleft interact with the C-terminal carboxylate (COO⁻) of the subunit at the end of the F strand, anchoring it in the cleft and properly positioning the F strand in relation to the chaperone G₁ strand.
 (B) Topology model of three subunits in a pilus tip fibrillum. Arrows indicate strands. Each subunit donates its N-terminal extension (red) to complete the immunoglobulin-like fold of the preceding subunit in the pilus. Diagonal lines indicate additional protein not shown.

position corresponding to Phe 138 is likewise conserved (Soto and Hultgren, 1999). The steric complementarity of these two residues in particular defines the proper register of the N-terminal extension in the groove.

The Chaperone Primes the Subunit by Maintaining the Groove in an Open, Activated Conformation

The reversal in orientation and shift in register of the complementing strands during donor strand exchange trigger a conformational change in the subunit groove, from an open to a closed state (Figures 3A, 4A, and 5). In the PapD_{His}PapE_{Ntd} chaperone-subunit complex, the C-terminal portion of the chaperone G₁ strand curves away from the groove, pulling with it the parallel F strand of PapE_{Ntd} and holding this end of the groove in an open conformation (Figures 3A, 4A, and 5A). In the PapE_{Ntd}K_{Nte} subunit-peptide complex, the reversal in orientation and shift in register in the complementing strands leaves nothing to replace the C-terminal portion of the G₁ strand at this end of the groove. The groove thus closes as the A1 and F strands on either side move closer together and the F strand makes additional interactions with the C strand (Figures 3A, 4A [compare the positions of the N termini and C termini of the PapE_{Ntd} structures], and 5B). The closing of the groove fills P1, leaving the N-terminal extension to interact with P2-P5 and clamps the N-terminal extension in place (Figure 5B). The resulting snug fit of the N-terminal extension in the closed groove presumably contributes to the relative stability of subunit-subunit interactions in the pilus and prevents further donor strand exchange (Figures 1C, 5C, and 5D). Donor strand exchange only occurs when the groove is held in the open conformation, that is, when the chaperone

is bound to the subunit (Figure 1C, lane 1). The chaperone thus primes the subunit for donor strand exchange by holding it in an open, activated state.

An Integrated View of Chaperone Function in Pilus Fiber Formation

These results provide an integrated, dynamic view of the mechanism of chaperone-assisted pilus fiber formation at high resolution. The chaperone initially prevents non-productive interactions of the pilus subunit by facilitating its proper folding and transiently capping its interactive groove (Kuehn et al., 1991; Jones et al., 1997; Barnhart et al., 2000). At the same time, as we demonstrate here, the chaperone primes the subunit for donor strand exchange by maintaining the subunit groove in an open, activated state. It is the characteristic non-canonical parallel orientation of the G_1 strand in the subunit groove in donor strand complementation that simultaneously accomplishes these apparently distinct functions of the chaperone. The C-terminal carboxylate at the end of the subunit F strand is anchored in the cleft between the two domains of the chaperone by interactions with the conserved Arg 8 and Lys 112 residues of the chaperone (Figure 6A) (Kuehn et al., 1993; Soto et al., 1998; Choudhury et al., 1999; Sauer et al., 1999). This anchoring interaction, which is required for the efficient formation of chaperone-subunit complexes, has been suggested to contribute to the proper positioning of the subunit F strand during subunit folding and capping (Slonim et al., 1992; Kuehn et al., 1993; Soto et al., 1998; Choudhury et al., 1999; Sauer et al., 2000). The anchoring interaction is a consequence of the parallel orientation of the chaperone G_1 and subunit F strands and would not occur were the orientation reversed, since the C-terminal carboxylate of the subunit F strand would no longer be in the cleft of the chaperone. Likewise, it has been shown here that the maintenance of the groove in an open conformation is also a consequence of the parallel orientation of the G_1 strand (Figures 3A and 4A). Were the orientation of the G_1 strand reversed, as is the case with N-terminal extension after donor strand exchange, the groove would close and the subunit would no longer be able to undergo donor strand exchange. Thus, the parallel orientation of the chaperone G_1 strand that characterizes donor strand complementation simultaneously accounts for folding, transient capping, and priming functions of the chaperone.

The chaperone thus couples the productive folding of the subunit with the transient capping of its interactive groove but maintains the subunit in an activated state, primed for donor strand exchange. The priming of the subunit permits its topological transition from a non-canonical to a canonical Ig fold during donor strand exchange. It is only after donor strand exchange, when the groove is closed and the N-terminal extension has completed the subunit Ig fold in a canonical manner, that the subunit attains its final topological, ground state as part of the mature pilus fiber. The chaperone thus makes possible the topological transition from an open, non-canonical Ig fold to a closed, perfectly canonical Ig fold that drives pilus fiber formation. Each subunit then contributes a strand to complete the fold of its neighbor to produce a very stable fiber (Figure 6B). The

elucidation of this mechanism sheds light both on the pathogenesis of many bacterial diseases and on the fundamental biological processes of chaperone function and fiber formation. The work thus promises to guide the development of new human therapeutics to treat bacterial infections and other human diseases characterized by pathogenic fiber formation.

Experimental Procedures

Protein Purification and In Vitro Donor Strand Exchange

PapE_{Ntd} (lacking residues 2–12 compared to wild-type PapE, which has 149 residues) was constructed and cloned into the pTrc99A expression plasmid (Amersham) using standard molecular biology techniques and coexpressed with PapD_{His} (plasmid pDF1) in *E. coli*. The periplasmic fraction was isolated and subjected to nickel and cation exchange chromatography (HiTrap Chelating and Source 15S media [Amersham]) to yield pure PapD_{His}PapE_{Ntd}. PapD_{His}PapK was isolated and purified in a similar fashion from *E. coli* harboring plasmids pDF1 and pFJ11 (Jacob-Dubuisson et al., 1993). PapE_{Ntd}K_{Nte} was obtained by incubating an ~15-fold molar excess of K_{Nte} peptide (residues 1–11 of the mature protein [Genemed Synthesis]) with PapD_{His}PapE_{Ntd} on ice for 3–4 hr and subjecting the mixture to nickel chromatography. The flowthrough contained pure PapE_{Ntd}K_{Nte}. For the gel in Figure 1C, an ~2-fold molar excess of PapD_{His}PapK was added to approximately equimolar amounts of either PapD_{His}PapE_{Ntd} or PapE_{Ntd}K_{Nte} and incubated overnight at 4°C before preparation of the samples for SDS-PAGE.

Crystallization

Seleno-methionylated (SeMet) PapD_{His}PapE_{Ntd} was produced in an *E. coli* methionine auxotroph (strain DL41) grown in medium containing selenomethionine. SeMet PapD_{His}PapE_{Ntd} and SeMet PapE_{Ntd}K_{Nte} were purified in the presence of 1 mM β -mercaptoethanol (β ME). Crystals of SeMet PapD_{His}PapE_{Ntd} (O.D.₂₈₀ 12–16) were grown by vapor diffusion using either the sitting or hanging drop method with a reservoir containing 100 mM Tris [pH 8.5], 250 mM MgCl₂, 17%–18% PEG 4000, and 4%–7% glycerol. Crystals formed in the space group P1 with $a = 55.9 \text{ \AA}$, $b = 56.7 \text{ \AA}$, $c = 60.9 \text{ \AA}$, $\alpha = 108.2^\circ$, $\beta = 89.9^\circ$, and $\gamma = 104.0^\circ$, and 2 complexes per asymmetric unit. Crystals of SeMet PapE_{Ntd}K_{Nte} (O.D.₂₈₀ 10–20) were grown by vapor diffusion using the hanging drop method with a reservoir containing 100 mM Tris 8.5, 200 mM NaCl, 27%–32% PEG 4000, and 1 mM β ME. Crystals formed in the space group P2₁ with $a = 25.2 \text{ \AA}$, $b = 91.9 \text{ \AA}$, $c = 51.2 \text{ \AA}$, and $\beta = 99.3 \text{ \AA}$, and 2 complexes per asymmetric unit. All crystals were flash-cooled in liquid nitrogen before data collection.

Structure Determination

Data were reduced and processed using DENZO, SCALEPACK, and HKL2000 (Otwinowski, 1993; Otwinowski and Minor, 1997). For PapD_{His}PapE_{Ntd}, a single-wavelength data set and a three-wavelength MAD data set were collected. The positions of 10 of the 12 selenium atoms in the asymmetric unit were determined and used to calculate MAD phases, and a density-modified electron density map was calculated (SOLVE [Terwilliger and Berendzen, 1999], RESOLVE [Terwilliger, 2000], and CNS [Brünger et al., 1998]). PapD_{His} was initially placed in the density by molecular replacement (AMORE [Navaza, 1994]). PapE_{Ntd} was built into the remaining density (O [Jones et al., 1991]), and the model was refined against the single-wavelength data set (CNS). A total of 86.7% of the residues are in the most favored region of the Ramachandran plot; none are in the disallowed region. The model contains residues 1–215 of both molecules of PapD_{His} in the asymmetric unit. One molecule of PapE_{Ntd} in the asymmetric unit contains residues 1, 13–28, 35–72, 78–127, and 137–149, with Glu 28 and Lys 108 built as alanines. The second molecule of PapE_{Ntd} contains residues 1, 13–24, 39–72, 81–127, and 137–149, with Gln 72, Lys 108, and Tyr 126 built as alanines. There was no interpretable density for atoms not built. For PapE_{Ntd}K_{Nte}, data was collected at the selenium peak. The positions of all 6 selenium atoms in the asymmetric unit were determined and used to calculate SAD phases (CNS). A prominent translation vector peak

relating the two complexes in the asymmetric unit and visible in the anomalous difference Patterson map facilitated the identification of the selenium positions. A density-modified electron density map was calculated (CNS) and $\text{PapE}_{\text{Nrd}}\text{K}_{\text{Nrd}}$ built into the density (O). The model was refined against a data set collected at a high-energy remote wavelength (CNS). A total of 92.1% of the residues are in the most favored region of the Ramachandran plot; none are in the disallowed region. In the model, one complex is complete, in the second, residues 78–79 of PapE_{Nrd} were not built. Figures were generated with RIBBONS (Carson, 1997) and GRASP (Nicholls et al., 1991).

Acknowledgments

We thank the staff at the SBC-CAT at the Advanced Photon Source at Argonne for their generous help during data collection. F.G.S. was supported by a National Science Foundation Predoctoral Fellowship. This work was supported by NIH grants RO1GM54033, RO1GM60231, and RO1AI49950 to G.W. and RO1DK51406, RO1AI29549, and RO1AI48689 to S.J.H.

Received: June 25, 2002

Revised: August 30, 2002

References

- Barnhart, M.M., Pinkner, J.S., Soto, G.E., Sauer, F.G., Langermann, S., Waksman, G., Frieden, C., and Hultgren, S.J. (2000). PapD-like chaperones provide the missing information for folding of pilin proteins. *Proc. Natl. Acad. Sci. USA* **97**, 7709–7714.
- Brünger, A.T., Adams, P.D., Clore, G.M., DeLano, W.L., Gros, P., Grosse-Kunstleve, R.W., Jiang, J.S., Kuszewski, J., Nilges, M., Pannu, N.S., et al. (1998). Crystallography and NMR system: a new software suite for macromolecular structure determination. *Acta Crystallogr. D54*, 905–921.
- Bullitt, E., and Makowski, L. (1995). Structural polymorphism of bacterial adhesion pili. *Nature* **373**, 164–167.
- Carson, M. (1997). Ribbons. *Methods Enzymol.* **277**, 493–505.
- Choudhury, D., Thompson, A., Stojanoff, V., Langermann, S., Pinkner, J., Hultgren, S.J., and Knight, S.D. (1999). X-ray structure of the FimC-FimH chaperone-adhesin complex from uropathogenic *Escherichia coli*. *Science* **285**, 1061–1066.
- Connell, H., Agace, W., Klemm, P., Schembri, M., Marild, S., and Svanborg, C. (1996). Type 1 fimbrial expression enhances *Escherichia coli* virulence for the urinary tract. *Proc. Natl. Acad. Sci. USA* **93**, 9827–9832.
- Dodson, K.W., Pinkner, J.S., Rose, T., Magnusson, G., Hultgren, S.J., and Waksman, G. (2001). Structural basis of the interaction of the pyelonephritic *E. coli* adhesin to its human kidney receptor. *Cell* **105**, 733–743.
- Gong, M., and Makowski, L. (1992). Helical structure of P pili from *Escherichia coli*. Evidence from X-ray fiber diffraction and scanning transmission electron microscopy. *J. Mol. Biol.* **228**, 735–742.
- Hardy, J., and Selkoe, D.J. (2002). The amyloid hypothesis of Alzheimer's disease: progress and problems on the road to therapeutics. *Science* **297**, 353–356.
- Hartl, F.U., and Hayer-Hartl, M. (2002). Molecular chaperones in the cytosol: from nascent chain to folded protein. *Science* **295**, 1852–1858.
- Hooton, T.M. (2000). Epidemiology. In *Urinary Tract Infection in the Female*, S.L. Stanton and P. L. Dwyer, eds. (London: Martin Dunitz), pp. 1–14.
- Hull, R.A., Gill, R.E., Hsu, P., Minshew, B.H., and Falkow, S. (1981). Construction and expression of recombinant plasmids encoding type 1 or D-mannose-resistant pili from a urinary tract infection *Escherichia coli* isolate. *Infect. Immun.* **33**, 933–938.
- Hultgren, S.J., Jones, C.H., and Normark, S.N. (1996). Bacterial adhesins and their assembly. In *Escherichia Coli and Salmonella; Cellular and Molecular Biology*, F.C. Neidhardt, ed. (Washington, D.C.: ASM Press), pp. 2730–2756.
- Hung, D.L., Knight, S.D., Woods, R.M., Pinkner, J.S., and Hultgren, S.J. (1996). Molecular basis of two subfamilies of immunoglobulin-like chaperones. *EMBO J.* **15**, 3792–3805.
- Hung, D.L., Raivio, T.L., Jones, C.H., Silhavy, T.J., and Hultgren, S.J. (2001). Cpx signaling pathway monitors biogenesis and affects assembly and expression of P pili. *EMBO J.* **20**, 1508–1518.
- Jacob-Dubuisson, F., Heuser, J., Dodson, K., Normark, S., and Hultgren, S.J. (1993). Initiation of assembly and association of the structural elements of a bacterial pilus depend on two specialized tip proteins. *EMBO J.* **12**, 837–847.
- Jones, T.A., Zou, J.Y., Cowan, S.W., and Kjeldgaard, M. (1991). Improved methods for building protein models in electron density maps and the location of errors in these models. *Acta Crystallogr. A47*, 110–119.
- Jones, C.H., Danese, P.N., Pinkner, J.S., Silhavy, T.J., and Hultgren, S.J. (1997). The chaperone-assisted membrane release and folding pathway is sensed by two signal transduction systems. *EMBO J.* **16**, 6394–6406.
- Kuehn, M.J., Normark, S., and Hultgren, S.J. (1991). Immunoglobulin-like PapD chaperone caps and uncaps interactive surfaces of nascently translocated pilus subunits. *Proc. Natl. Acad. Sci. USA* **88**, 10586–10590.
- Kuehn, M.J., Heuser, J., Normark, S., and Hultgren, S.J. (1992). P pili in uropathogenic *E. coli* are composite fibres with distinct fibrillar adhesive tips. *Nature* **356**, 252–255.
- Kuehn, M.J., Ogg, D.J., Kihlberg, J., Slonim, L.N., Flemmer, K., Bergfors, T., and Hultgren, S.J. (1993). Structural basis of pilus subunit recognition by the PapD chaperone. *Science* **262**, 1234–1241.
- Lindberg, F., Tennent, J.M., Hultgren, S.J., Lund, B., and Normark, S. (1989). PapD, a periplasmic transport protein in P-pilus biogenesis. *J. Bacteriol.* **171**, 6052–6058.
- Lund, B., Lindberg, F., Marklund, B.I., and Normark, S. (1987). The PapG protein is the α -D-galactopyranosyl-(1–4)- β -D-galactopyranose-binding adhesin of uropathogenic *Escherichia coli*. *Proc. Natl. Acad. Sci. USA* **84**, 5898–5902.
- Martinez, J.J., Mulvey, M.A., Schilling, J.D., Pinkner, J.S., and Hultgren, S.J. (2000). Type 1 pilus-mediated bacterial invasion of bladder epithelial cells. *EMBO J.* **19**, 2803–2812.
- Muhldorfer, I., Ziebuhr, W., and Hacker, J. (2001). *Escherichia coli* in urinary tract infections. In *Molecular Medical Microbiology*, M. Sussman, ed. (San Diego: Academic Press), pp. 1515–1540.
- Mulvey, M.A., Lopez-Boado, Y.S., Wilson, C.L., Roth, R., Parks, W.C., Heuser, J., and Hultgren, S.J. (1998). Induction and evasion of host defenses by type 1-piliated uropathogenic *Escherichia coli*. *Science* **282**, 1494–1497.
- Navaza, J. (1994). AMoRe: an automated package for molecular replacement. *Acta Crystallogr. A50*, 157–163.
- Nicholls, A., Sharp, K.A., and Honig, B. (1991). Protein folding and association: insights from the interfacial and thermodynamic properties of hydrocarbons. *Proteins* **11**, 281–296.
- Otwinowski, Z. (1993). Oscillation data reduction program. In *Proceedings of the CCP4 study weekend: data collection and processing*, L. Sawyers, N. Isaacs, and S. Bailey, eds. (Warrington: SERC Daresbury Laboratory), pp. 56–62.
- Otwinowski, Z., and Minor, W. (1997). Processing of X-ray diffraction data collected in oscillation mode. *Methods Enzymol.* **276**, 307–326.
- Roberts, J.A., Marklund, B.I., Ilver, D., Haslam, D., Kaack, M.B., Baskin, G., Louis, M., Mollby, R., Winberg, J., and Normark, S. (1994). The Gal(α 1–4)Gal-specific tip adhesin of *Escherichia coli* P-fimbriae is needed for pyelonephritis to occur in the normal urinary tract. *Proc. Natl. Acad. Sci. USA* **91**, 11889–11893.
- Sauer, F.G., Futterer, K., Pinkner, J.S., Dodson, K.W., Hultgren, S.J., and Waksman, G. (1999). Structural basis of chaperone function and pilus biogenesis. *Science* **285**, 1058–1061.
- Sauer, F.G., Knight, S.D., Waksman, G., and Hultgren, S.J. (2000). PapD-like chaperones and pilus biogenesis. *Semin. Cell Dev. Biol.* **11**, 27–34.
- Saulino, E.T., Bullitt, E., and Hultgren, S.J. (2000). Snapshots of

usher-mediated protein secretion and ordered pilus assembly. *Proc. Natl. Acad. Sci. USA* 97, 9240–9245.

Slonim, L.N., Pinkner, J.S., Branden, C.I., and Hultgren, S.J. (1992). Interactive surface in the PapD chaperone cleft is conserved in pilus chaperone superfamily and essential in subunit recognition and assembly. *EMBO J.* 11, 4747–4756.

Soto, G.E., and Hultgren, S.J. (1999). Bacterial adhesins: common themes and variations in architecture and assembly. *J. Bacteriol.* 181, 1059–1071.

Soto, G.E., Dodson, K.W., Ogg, D., Liu, C., Heuser, J., Knight, S., Kihlberg, J., Jones, C.H., and Hultgren, S.J. (1998). Periplasmic chaperone recognition motif of subunits mediates quaternary interactions in the pilus. *EMBO J.* 17, 6155–6167.

Stanton, S.L., and Dwyer, P.L. (2000). Preface. In *Urinary Tract Infection in the Female*, S.L. Stanton and P. L. Dwyer, eds. (London: Martin Dunitz), pp. xi–xii.

Stebbins, C.E., and Galan, J.E. (2001). Maintenance of an unfolded polypeptide by a cognate chaperone in bacterial type III secretion. *Nature* 414, 77–81.

Striker, R., Jacob-Dubuisson, F., Freiden, C., and Hultgren, S.J. (1994). Stable fiber-forming and nonfiber-forming chaperone-subunit complexes in pilus biogenesis. *J. Biol. Chem.* 269, 12233–12239.

Sussman, M. (2001). Urinary tract infections: a clinical overview. In *Molecular Medical Microbiology*, M. Sussman, ed. (San Diego: Academic Press), pp. 1507–1513.

Terwilliger, T.C. (2000). Maximum likelihood density modification. *Acta Crystallogr. D Biol. Crystallogr.* 56, 965–972.

Terwilliger, T.C., and Berendzen, J. (1999). Automated MAD and MIR structure solution. *Acta Crystallogr. D Biol. Crystallogr.* 55, 849–861.

Thanassi, D.G., Saulino, E.T., and Hultgren, S.J. (1998a). The chaperone/usher pathway: a major terminal branch of the general secretory pathway. *Curr. Opin. Microbiol.* 1, 223–231.

Thanassi, D.G., Saulino, E.T., Lombardo, M.J., Roth, R., Heuser, J., and Hultgren, S.J. (1998b). The PapC usher forms an oligomeric channel: implications for pilus biogenesis across the outer membrane. *Proc. Natl. Acad. Sci. USA* 95, 3146–3151.

Warren, J. (1996). Clinical presentations and epidemiology of urinary tract infections. In *Urinary Tract Infections: Molecular Pathogenesis and Clinical Management*, H.L.T. Mobley, and J. W. Warren, eds. (Washington, D.C.: ASM Press), pp. 3–27.

Accession Numbers

Coordinates for PapD_{HIS}PapE_{Ntd} (1N0L) and for PapE_{Ntd}K_{Nte} (1N1Z) have been deposited at the Protein Data Bank.